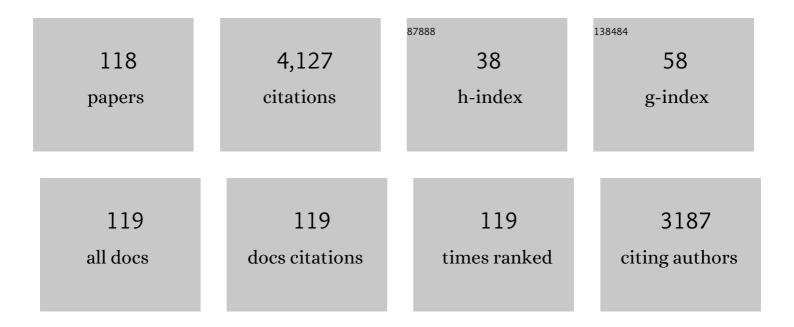
List of Publications by Year in descending order

Source: https://exaly.com/author-pdf/6941230/publications.pdf Version: 2024-02-01



#	Article	IF	CITATIONS
1	Engineering anion defect in perovskite oxyfluoride cathodes enables proton involved oxygen reduction reaction for protonic ceramic fuel cells. Separation and Purification Technology, 2022, 290, 120844.	7.9	23
2	Nonnoble metal oxides for highâ€performance Znâ€air batteries: Design strategies and future challenges. Asia-Pacific Journal of Chemical Engineering, 2022, 17, .	1.5	2
3	Developing a Unique Hydrogen-Bond Network in a Uranyl Coordination Framework for Fuel Cell Applications. Inorganic Chemistry, 2022, 61, 8036-8042.	4.0	8
4	In-situ construction of Ruddlesden-Popper/perovskite heterointerface induces efficient bifunctional oxygen electrocatalyst for rechargeable zinc-air batteries. Electrochimica Acta, 2022, 424, 140673.	5.2	10
5	Realizing robust and efficient acidic oxygen evolution by electronic modulation of 0D/2D CeO2 quantum dots decorated SrIrO3 nanosheets. Applied Catalysis B: Environmental, 2022, 315, 121579.	20.2	28
6	Enhancing the bifunctional activity of CoSe2 nanocubes by surface decoration of CeO2 for advanced zinc-air batteries. Journal of Colloid and Interface Science, 2022, 625, 839-849.	9.4	14
7	Probing oxygen reduction and water uptake kinetics of BaCo0.4Fe0.4Zr0.1Y0.1-xZnxO3-δ cathodes for protonic ceramic fuel cells. Separation and Purification Technology, 2022, 297, 121482.	7.9	18
8	Metal organic framework derived perovskite/spinel heterojunction as efficient bifunctional oxygen electrocatalyst for rechargeable and flexible Zn-air batteries. Journal of Colloid and Interface Science, 2022, 625, 502-511.	9.4	21
9	FeS2–CoS2 incorporated into nitrogen-doped carbon nanofibers to boost oxygen electrocatalysis for durable rechargeable Zn-air batteries. Journal of Power Sources, 2021, 482, 228955.	7.8	67
10	Free volume dependence of dielectric behaviour in sandwich-structured high dielectric performances of poly(vinylidene fluoride) composite films. Nanoscale, 2021, 13, 300-310.	5.6	26
11	In-situ exsolution of CoNi alloy nanoparticles on LiFe0.8Co0.1Ni0.1O2 parent: New opportunity for boosting oxygen evolution and reduction reaction. Applied Surface Science, 2021, 543, 148817.	6.1	24
12	Tuning the Oxygen Vacancy of the SrSc _{0.175} Nb _{0.025} Co _{0.8} O _{3â^ʾÎ} Cathode toward Enhanced Oxygen Reduction Reaction for H ⁺ -SOFCs by Water Uptake. Energy & Fuels, 2021, 35, 8953-8960.	5.1	10
13	In-situ photodeposition of CoSx on Pa0.5Ba0.5Mn0.25Fe0.75O3-δ perovskite to boost bifunctional oxygen electrocatalysis for rechargeable Zn-air batteries. Electrochimica Acta, 2021, 391, 138951.	5.2	10
14	Silver decorated cobalt carbonate to enable high bifunctional activity for oxygen electrocatalysis and rechargeable Zn-air batteries. Journal of Colloid and Interface Science, 2021, 603, 252-258.	9.4	17
15	Electronic tuning of SrIrO3 perovskite nanosheets by sulfur incorporation to induce highly efficient and long-lasting oxygen evolution in acidic media. Applied Catalysis B: Environmental, 2021, 298, 120562.	20.2	55
16	Hierarchical iron-phosphide@NiCo2O4 nanoneedle arrays for high performance water splitting. Applied Surface Science, 2021, 569, 151016.	6.1	8
17	Integrated Ultrafine Co _{0.85} Se in Carbon Nanofibers: An Efficient and Robust Bifunctional Catalyst for Oxygen Electrocatalysis. Chemistry - A European Journal, 2020, 26, 4063-4069.	3.3	25
18	Investigation of Fe-substituted in BaZr0.8Y0.2O3-δ proton conducting oxides as cathode materials for protonic ceramics fuel cells. Journal of Alloys and Compounds, 2020, 814, 152220.	5.5	28

#	Article	IF	CITATIONS
19	High efficiency and selectivity from synergy: Bi nanoparticles embedded in nitrogen doped porous carbon for electrochemical reduction of CO2 to formate. Electrochimica Acta, 2020, 334, 135563.	5.2	37
20	<i>In situ</i> exsolved Co nanoparticles coupled on LiCoO ₂ nanofibers to induce oxygen electrocatalysis for rechargeable Zn–air batteries. Journal of Materials Chemistry A, 2020, 8, 19946-19953.	10.3	27
21	Modified carbon fiber electrodes with enhanced impedance performance for marine sensor. Journal of the Taiwan Institute of Chemical Engineers, 2020, 109, 137-144.	5.3	3
22	Tuning Nanofillers in In Situ Prepared Polyimide Nanocomposites for Highâ€Temperature Capacitive Energy Storage. Advanced Energy Materials, 2020, 10, 1903881.	19.5	259
23	Ag-modified carbon fiber as a stable sensor. Composites Part A: Applied Science and Manufacturing, 2020, 137, 106034.	7.6	6
24	Oxygen vacancies-rich Ce0.9Gd0.1O2-δ decorated Pr0.5Ba0.5CoO3-δ bifunctional catalyst for efficient and long-lasting rechargeable Zn-air batteries. Applied Catalysis B: Environmental, 2020, 266, 118656.	20.2	87
25	Na incorporation controlled single phase kesterite Cu2ZnSnS4 solar cell material. Materials Letters, 2020, 265, 127355.	2.6	7
26	Coupling amorphous cobalt hydroxide nanoflakes on Sr ₂ Fe _{1.5} Mo _{0.5} O _{5+δ} perovskite nanofibers to induce bifunctionality for water splitting. Nanoscale, 2020, 12, 9048-9057.	5.6	33
27	Lead and tungsten double stabilizing cobaltâ€based perovskite oxygen permeation membranes for clean energy delivery. International Journal of Energy Research, 2020, 44, 6259-6268.	4.5	2
28	Mobility Improvement of Sol–Gel Method Processed Transparent SnSx Thin Films by Na Doping. Journal of Nanoscience and Nanotechnology, 2020, 20, 5102-5106.	0.9	1
29	An integrated bifunctional catalyst of metal-sulfide/perovskite oxide for lithium-oxygen batteries. Journal of Power Sources, 2019, 437, 226908.	7.8	23
30	Carbon quantum dots decorated Ba0.5Sr0.5Co0.8Fe0.2O3- perovskite nanofibers for boosting oxygen evolution reaction. Applied Catalysis B: Environmental, 2019, 257, 117919.	20.2	79
31	Engineering anion defect in LaFeO2.85Cl0.15 perovskite for boosting oxygen evolution reaction. International Journal of Hydrogen Energy, 2019, 44, 24077-24085.	7.1	26
32	SnSe ₂ Nanorods on Carbon Cloth as a Highly Selective, Active, and Flexible Electrocatalyst for Electrochemical Reduction of CO ₂ into Formate. ACS Applied Energy Materials, 2019, 2, 7655-7662.	5.1	39
33	Co 3+ â€Rich Na 1.95 CoP 2 O 7 Phosphates as Efficient Bifunctional Catalysts for Oxygen Evolution and Reduction Reactions in Alkaline Solution. Chemistry - A European Journal, 2019, 25, 11007-11014.	3.3	12
34	Plasma engraved Bi0.1(Ba0.5Sr0.5)0.9Co0.8Fe0.2O3â~δ perovskite for highly active and durable oxygen evolution. Scientific Reports, 2019, 9, 4210.	3.3	20
35	Strategic hierarchical improvement of superprotonic conductivity in a stable metal–organic framework system. Journal of Materials Chemistry A, 2019, 7, 25165-25171.	10.3	76
36	Insights into Ni-Fe couple in perovskite electrocatalysts for highly efficient electrochemical oxygen evolution. Electrochimica Acta, 2019, 293, 240-246.	5.2	30

#	Article	IF	CITATIONS
37	Lanthanum modified lead zirconate titanate thin films by sol-gel and plasma annealing for integrated passive nanophotonic devices. Optical Materials Express, 2019, 9, 2279.	3.0	3
38	Unique Proton Transportation Pathway in a Robust Inorganic Coordination Polymer Leading to Intrinsically High and Sustainable Anhydrous Proton Conductivity. Journal of the American Chemical Society, 2018, 140, 6146-6155.	13.7	181
39	(Pr 0.9 La 0.1) 2 (Ni 0.74 Cu 0.21 Nb 0.05)O 4+l̂´-Ce 0.9 Gd 0.1 O 2â ^{-s} l̂´ (GDC) as an active and CO 2 -tolerant nano-composite cathode for intermediate temperature solid oxide fuel cells. International Journal of Hydrogen Energy, 2018, 43, 3291-3298.	7.1	14
40	Structure dependence of water vapor permeation in polymer nanocomposite membranes investigated by positron annihilation lifetime spectroscopy. Journal of Membrane Science, 2018, 549, 581-587.	8.2	52
41	Boosting Overall Water Splitting via FeOOH Nanoflake-Decorated PrBa _{0.5} Sr _{0.5} Co ₂ O _{5+δ} Nanorods. ACS Applied Materials & Interfaces, 2018, 10, 38032-38041.	8.0	66
42	Nickelâ€Based Bicarbonates as Bifunctional Catalysts for Oxygen Evolution and Reduction Reaction in Alkaline Media. Chemistry - A European Journal, 2018, 24, 17665-17671.	3.3	15
43	Copper nanowires/cellulose biodegradable flexible transparent conductor with improved thermal stability and its application. Organic Electronics, 2018, 63, 392-397.	2.6	7
44	Atomic layered deposition iron oxide on perovskite LaNiO3 as an efficient and robust bi-functional catalyst for lithium oxygen batteries. Electrochimica Acta, 2018, 281, 338-347.	5.2	57
45	Partially reduced Sn/SnO2 porous hollow fiber: A highly selective, efficient and robust electrocatalyst towards carbon dioxide reduction. Electrochimica Acta, 2018, 285, 70-77.	5.2	51
46	Enhanced Electrochemical Activity and Chromium Tolerance of the Nucleation-Agent-Free La2Ni0.9Fe0.1O4+l̂´Cathode by Gd0.1Ce0.9O1.95 Incorporation. Electronic Materials Letters, 2018, 14, 432-439.	2.2	6
47	Flexible Transparent Conductive Au/Polythiophene/Cellulose Sheet. Nanoscience and Nanotechnology Letters, 2018, 10, 108-111.	0.4	2
48	Effect of Co doping on sinterability and protonic conductivity of BaZr0.1Ce0.7Y0.1Yb0.1O3â~δfor protonic ceramic fuel cells. Journal of Power Sources, 2017, 347, 14-20.	7.8	48
49	Synthesis and magnetoelectric properties of multiferroic composites of lead lanthanum zirconate titanate and mesoporous cobalt ferrite. Scripta Materialia, 2017, 136, 29-32.	5.2	14
50	An active functional layer for carbon-tolerant anode of intermediate temperature solid oxide fuel cells. Materials Letters, 2017, 208, 54-57.	2.6	11
51	Novel, cobalt-free, and highly active Sr2Fe1.5Mo0.5â^'xSnxO6â^'Î^ cathode materials for intermediate temperature solid oxide fuel cells. International Journal of Hydrogen Energy, 2017, 42, 10308-10316.	7.1	26
52	The effect of the Zn/Sn ratio on the formation of single phase kesterite Cu 2 ZnSnS 4 solar cell material. Ceramics International, 2017, 43, 8103-8108.	4.8	10
53	A novel layered perovskite as symmetric electrode for direct hydrocarbon solid oxide fuel cells. Journal of Power Sources, 2017, 342, 313-319.	7.8	89
54	Application of a novel (Pr0.9La0.1)2(Ni0.74Cu0.21Nb0.05)O4+δ-infiltrated BaZr0.1Ce0.7Y0.2O3-δ cathode for high performance protonic ceramic fuel cells. Journal of Power Sources, 2017, 341, 192-198.	7.8	60

#	Article	IF	CITATIONS
55	Numerical modeling of ceria-based SOFCs with bi-layer electrolyte free from internal short circuit: Comparison of two cell configurations. Electrochimica Acta, 2017, 248, 356-367.	5.2	22
56	Formaldehyde assisted reduction achieved p-type orthorhombic tin oxide film prepared by an inexpensive chemical method. Materials Research Express, 2017, 4, 116411.	1.6	2
57	Effect of preparation process on properties of PLZT (9/65/35) transparent ceramics. Journal of Alloys and Compounds, 2017, 723, 602-610.	5.5	25
58	Improved mobility of sol-gel method processed transparent tin sulfide thin films. Materials Letters, 2016, 178, 231-234.	2.6	13
59	Sm0.5Sr0.5CoO3â^'δ infiltrated Ce0.9Gd0.1O2â^`δ composite cathodes for high performance protonic ceramic fuel cells. Journal of Power Sources, 2016, 333, 24-29.	7.8	24
60	A comparison study of chromium deposition and poisoning on La0.8Sr0.2Ga0.8Mg0.2O3â^î^´ and Gd0.1Ce0.9O2â^î^´ electrolytes of solid oxide fuel cells. Journal of Alloys and Compounds, 2016, 688, 376-381.	5.5	8
61	Glucose-assisted reduction achieved transparent p-type cuprous oxide thin film by a solution method. Europhysics Letters, 2016, 115, 37005.	2.0	6
62	Bismuth and indium co-doping strategy for developing stable and efficient barium zirconate-based proton conductors for high-performance H-SOFCs. Journal of the European Ceramic Society, 2016, 36, 3423-3431.	5.7	52
63	Antimony doped barium strontium ferrite perovskites as novel cathodes for intermediate-temperature solid oxide fuel cells. Journal of Alloys and Compounds, 2016, 666, 23-29.	5.5	36
64	Tailoring of surface modified ultrathin membranes with CO ₂ tolerance and high oxygen permeability. Journal of Materials Chemistry A, 2016, 4, 4003-4008.	10.3	20
65	Enhanced Oxygen Permeation Behavior of Ba _{0.5} Sr _{0.5} Co _{0.8} Fe _{0.2} O _{3â^{~1}Î} Membranes in a CO ₂ -Containing Atmosphere with a Sm _{0.2} Ce _{0.8} O _{1.9} Functional Shell. Energy & amp; Fuels, 2016, 30, 1829-1834.	5.1	17
66	Probing novel triple phase conducting composite cathode for high performance protonic ceramic fuel cells. International Journal of Hydrogen Energy, 2016, 41, 5074-5083.	7.1	30
67	Enhanced sinterability and conductivity of BaZr0.3Ce0.5Y0.2O3â~δ by addition of bismuth oxide for proton conducting solid oxide fuel cells. Journal of Power Sources, 2016, 301, 369-375.	7.8	43
68	A new, high electrochemical activity and chromium tolerant cathode for solid oxide fuel cells. International Journal of Hydrogen Energy, 2015, 40, 15622-15631.	7.1	17
69	Synthesis and characterization of a Sr0.95Y0.05TiO3â^1̂-based hydrogen electrode for reversible solid oxide cells. RSC Advances, 2015, 5, 17000-17006.	3.6	4
70	Efficient modification for enhancing surface activity of Ba0.5Sr0.5Co0.8Fe0.2O3â~δ oxygen permeation membrane. Journal of Membrane Science, 2015, 477, 7-13.	8.2	24
71	Chromium deposition and poisoning at La _{0.6} Sr _{0.4} Co _{0.2} Fe _{0.8} O _{3â^îÎ} oxygen electrodes of solid oxide electrolysis cells. Physical Chemistry Chemical Physics, 2015, 17, 1601-1609.	2.8	52
72	Tailoring Electrochemical Property of Layered Perovskite Cathode by Cuâ€doping for Proton onducting IT‧OFCs. Fuel Cells, 2015, 15, 384-389.	2.4	20

#	Article	IF	CITATIONS
73	A comparison of oxygen permeation and CO2 tolerance of La0.6Sr0.4Co0.2Fe0.6Nb0.2O3â^ and La0.6Sr0.4Fe0.8Nb0.2O3â^ ceramic membranes. Journal of Alloys and Compounds, 2015, 644, 788-792.	5.5	9
74	New insight into highly active cathode of proton conducting solid oxide fuel cells by oxygen ionic conductor modification. Journal of Power Sources, 2015, 287, 170-176.	7.8	27
75	Highly active YSB infiltrated LSCF cathode for proton conducting solid oxide fuel cells. International Journal of Hydrogen Energy, 2015, 40, 13576-13582.	7.1	34
76	Fabrication and evaluation of stable micro tubular solid oxide fuel cells with BZCY-BZY bi-layer proton conducting electrolytes. International Journal of Hydrogen Energy, 2014, 39, 19087-19092.	7.1	24
77	Performance stability and degradation mechanism of La 0.6 Sr 0.4 Co 0.2 Fe 0.8 O 3â^î^ cathodes under solid oxide fuel cells operation conditions. International Journal of Hydrogen Energy, 2014, 39, 15868-15876.	7.1	85
78	Cathode supported tubular solid oxide fuel cells with nanostructured La0.6Sr0.4Co0.2Fe0.8O3 electrocatalysts. Journal of Power Sources, 2014, 266, 268-274.	7.8	6
79	Raman Spectroscopy Study of Chromium Deposition on La _{0.6} Sr _{0.4} Co _{0.2} Fe _{0.8} O _{3-δ} Cathode of Solid Oxide Fuel Cells. Journal of the Electrochemical Society, 2014, 161, F687-F693.	2.9	44
80	lnsight into surface segregation and chromium deposition on La _{0.6} Sr _{0.4} Co _{0.2} Fe _{0.8} O _{3â~î^} cathodes of solid oxide fuel cells. Journal of Materials Chemistry A, 2014, 2, 11114-11123.	10.3	128
81	The effect of Cr deposition and poisoning on BaZr 0.1 Ce 0.7 Y 0.2 O 3â~δ proton conducting electrolyte. International Journal of Hydrogen Energy, 2014, 39, 18379-18384.	7.1	10
82	Effect of temperature on the chromium deposition and poisoning of La0.6Sr0.4Co0.2Fe0.8O3-δ cathodes of solid oxide fuel cells. Electrochimica Acta, 2014, 139, 173-179.	5.2	39
83	Comparative study of electrochemical properties of different composite cathode materials associated to stable proton conducting BaZr 0.7 Pr 0.1 Y 0.2 O 3-δelectrolyte. Electrochimica Acta, 2014, 146, 1-7.	5.2	25
84	Study on the Cr deposition and poisoning phenomenon at (La 0.6 Sr 0.4)(Co 0.2 Fe 0.8)O 3â^δelectrode of solid oxide fuel cells by transmission X-ray microscopy. International Journal of Hydrogen Energy, 2014, 39, 15728-15734.	7.1	20
85	A surface modified La 0.6 Sr 0.4 Co 0.2 Fe 0.8 O 3â~ʾî´ ultrathin membrane for highly efficient oxygen separation. Journal of Membrane Science, 2014, 464, 55-60.	8.2	32
86	Effect of nickel impregnated hollow fiber anode for micro tubular solid oxide fuel cells. Journal of Power Sources, 2014, 258, 391-394.	7.8	8
87	Surface Segregation and Chromium Deposition and Poisoning on La0.6Sr0.4Co0.2Fe0.8O3-Â Cathodes of Solid Oxide Fuel Cells. ECS Transactions, 2013, 57, 599-604.	0.5	10
88	Boron Poisoning of (La, Sr)(Co, Fe)O3 Cathodes of Solid Oxide Fuel Cells. ECS Transactions, 2013, 57, 1821-1830.	0.5	1
89	SmBaCo ₂ O _{5+δ} as High Efficient Oxygen Electrode of Solid Oxide Electrolysis Cells. ECS Transactions, 2013, 57, 3189-3196.	0.5	8
90	Enhanced Chromium Tolerance of Gd0.1Ce0.9O1.95 Impregnated La0.6Sr0.4Co0.2Fe0.8O3-Â Electrode of Solid Oxide Fuel Cells. ECS Transactions, 2013, 57, 2163-2173.	0.5	1

#	Article	IF	CITATIONS
91	Effect of Boron Deposition and Poisoning on the Surface Exchange Properties of LSCF Electrode Materials of Solid Oxide Fuel Cells. Journal of the Electrochemical Society, 2013, 160, F682-F686.	2.9	35
92	Enhanced chromium tolerance of La0.6Sr0.4Co0.2Fe0.8O3â^1r´ electrode of solid oxide fuel cells by Gd0.1Ce0.9O1.95 impregnation. Electrochemistry Communications, 2013, 37, 84-87.	4.7	54
93	Potentiality of cobalt-free perovskite Ba0.5Sr0.5Fe0.9Mo0.1O3â~δas a single-phase cathode for intermediate-to-low-temperature solid oxide fuel cells. International Journal of Hydrogen Energy, 2013, 38, 14323-14328.	7.1	21
94	Ti-doped molybdenum-based perovskites as anodes for solid oxide fuel cells. Journal of Power Sources, 2013, 241, 627-633.	7.8	45
95	Effect of Volatile Boron Species on the Microstructure and Composition of (La,Sr)MnO3and (La,Sr)(Co,Fe)O3Cathode Materials of Solid Oxide Fuel Cells. Journal of the Electrochemical Society, 2013, 160, F1033-F1039.	2.9	19
96	Effect of Volatile Boron Species on the Electrocatalytic Activity of Cathodes of Solid Oxide Fuel Cells. Journal of the Electrochemical Society, 2013, 160, F301-F308.	2.9	32
97	Effect of Volatile Boron Species on the Electrocatalytic Activity of Cathodes of Solid Oxide Fuel Cells. Journal of the Electrochemical Society, 2013, 160, F183-F190.	2.9	30
98	Sr ₂ Fe _{1.5} Mo _{0.5} O _{6â^ʾÎ} - Sm _{0.2} Ce _{0.8} O _{1.9} Composite Anodes for Intermediate-Temperature Solid Oxide Fuel Cells. Journal of the Electrochemical Society, 2012, 159, B619-B626.	2.9	73
99	Reaction model for cathodes cooperated with oxygen-ion conductors for solid oxide fuel cells using proton-conducting electrolytes. International Journal of Hydrogen Energy, 2012, 37, 548-554.	7.1	42
100	A cobalt-free Sm0.5Sr0.5Fe0.8Cu0.2O3â^Îr–Ce0.8Sm0.2O2â^Îr composite cathode for proton-conducting solid oxide fuel cells. Journal of Power Sources, 2011, 196, 2631-2634.	7.8	66
101	Electro-catalytic activity of Dy2O3 as a solid oxide fuel cell anode material. Electrochemistry Communications, 2011, 13, 194-196.	4.7	19
102	BaZr0.1Ce0.7Y0.2O3â^î^ as an electronic blocking material for microtubular solid oxide fuel cells based on doped ceria electrolyte. Electrochemistry Communications, 2011, 13, 450-453.	4.7	27
103	Ni–LnOx (Ln=Dy, Ho, Er, Yb and Tb) cermet anodes for intermediate-temperature solid oxide fuel cells. Electrochimica Acta, 2011, 56, 7071-7077.	5.2	4
104	Synthesis, characterization and evaluation of PrBaCo2â^'xFexO5+l´ as cathodes for intermediate-temperature solid oxide fuel cells. International Journal of Hydrogen Energy, 2011, 36, 3658-3665.	7.1	144
105	Ni-Sm2O3 cermet anodes for intermediate-temperature solid oxide fuel cells with stabilized zirconia electrolytes. International Journal of Hydrogen Energy, 2011, 36, 5589-5594.	7.1	13
106	Micro-tubular solid oxide fuel cells with graded anodes fabricated with a phase inversion method. Journal of Power Sources, 2011, 196, 962-967.	7.8	44
107	Novel layered perovskite oxide PrBaCuCoO5+δas a potential cathode for intermediate-temperature solid oxide fuel cells. Journal of Power Sources, 2010, 195, 453-456.	7.8	60
108	Low-temperature solid oxide fuel cells with novel La0.6Sr0.4Co0.8Cu0.2O3â~̂δ perovskite cathode and functional graded anode. Journal of Power Sources, 2010, 195, 1624-1629.	7.8	29

#	Article	IF	CITATIONS
109	Electrochemical performance of novel cobalt-free oxide Ba0.5Sr0.5Fe0.8Cu0.2O3â~δ for solid oxide fuel cell cathode. Journal of Power Sources, 2010, 195, 1859-1861.	7.8	79
110	A cobalt-free SrFe0.9Sb0.1O3â^'î´ cathode material for proton-conducting solid oxide fuel cells with stable BaZr0.1Ce0.7Y0.1Yb0.1O3â^'î´ electrolyte. Journal of Power Sources, 2010, 195, 7042-7045.	7.8	48
111	Characterization and evaluation of NdBaCo2O5+Ĩ´ cathode for proton-conducting solid oxide fuel cells. International Journal of Hydrogen Energy, 2010, 35, 753-756.	7.1	48
112	Cobalt-free oxide Ba0.5Sr0.5Fe0.8Cu0.2O3â^^î^ for proton-conducting solid oxide fuel cell cathode. International Journal of Hydrogen Energy, 2010, 35, 3769-3774.	7.1	66
113	Investigation of cobalt-free cathode material Sm0.5Sr0.5Fe0.8Cu0.2O3â^î^ for intermediate temperature solid oxide fuel cell. International Journal of Hydrogen Energy, 2010, 35, 6905-6910.	7.1	93
114	Layered SmBaCuCoO5+ and SmBaCuFeO5+ perovskite oxides as cathode materials for proton-conducting SOFCs. Journal of Alloys and Compounds, 2010, 492, 291-294.	5.5	29
115	Layered perovskite LaBaCuMO5+x (M=Fe, Co) cathodes for intermediate-temperature protonic ceramic membrane fuel cells. Journal of Alloys and Compounds, 2010, 493, 252-255.	5.5	39
116	In situ drop-coated BaZr0.1Ce0.7Y0.2O3â^´Î´ electrolyte-based proton-conductor solid oxide fuel cells with a novel layered PrBaCuFeO5+δ cathode. Journal of Power Sources, 2009, 194, 291-294.	7.8	41
117	High performance of proton-conducting solid oxide fuel cell with a layered PrBaCo2O5+δ cathode. Journal of Power Sources, 2009, 194, 835-837.	7.8	109
118	High sintering ability and electrical conductivity of Zn doped La(Ca)CrO3 based interconnect ceramics for SOFCs. Journal of Power Sources, 2008, 177, 451-456.	7.8	18